MOEM

Modern Electronic Materials 2019; 5(3): 101–105
DOI 10.3897/j.moem.5.3.51573

Research Article

Effect of Ca^{2+} and Zr^{4+} co-doping on the optical properties of $Gd_3Al_2Ga_3O_{12}$: Ce single crystals

Valentina M. Kasimova[1], Nina S. Kozlova[1], Oleg A. Buzanov[2], Evgeniya V. Zabelina[1]

1 National University of Science and Technology «MISiS», Leninsky Prospekt 4, Moscow 119049, Russia

2 JSC Fomos-Materials, 16 Buzheninova Str., Moscow 107023, Russia

Corresponding author: Valentina M. Kasimova (kasimovavalya@mail.ru)

Received 28 March 2019 ♦ **Accepted** 19 June 2019 ♦ **Published** 12 September 2019

Citation: Kasimova VM, Kozlova NS, Buzanov OA, Zabelina EV (2019) Effect of Ca^{2+} and Zr^{4+} co-doping on the optical properties of $Gd_3Al_2Ga_3O_{12}$: Ce single crystals. Modern Electronic Materials 5(3): 101–105. https://doi.org/10.3897/j.moem.5.3.51573

Abstract

Scintillation materials capable of transforming absorbed high-energy particles into visible radiation photons find multiple applications including advanced medical visualization methods. $Gd_3Al_2Ga_3O_{12}$: Ce is a promising oxygen-containing scintillator for fabrication of detecting crystals of positron emission tomographs due to its unique properties, e.g. high density, high light yield, radiation hardness etc. However its kinetic parameters currently restrict its use in this field. Attempts at improving the luminescence rise and decay time kinetics by introducing additional impurities have become a top priority task for many researchers. Analyzing literary data one can conclude that the optical parameters of co-doped crystals have been studied insufficiently or have not been studied at all. We have studied Ca^{2+} and Zr^{4+} co-doped $Gd_3Al_2Ga_3O_{12}$: Ce single crystals by optical spectroscopy in the 200–2200 nm. We have taken the optical transmittance, absorption and reflection spectra and measured the refractive indices. Dispersion curves have been obtained by approximation of experimental refractive indices using the Brewster method and the Cauchy equation. Material constants of these equations have been estimated for each of the co-doped crystals.

Keywords

$Gd_3A_{12}Ga_3O_{12}$: Ce, scintillation single crystal, co-doping, transmittance spectrophotometry, absorption coefficient, refractive index, Brewster method, approximation

1. Introduction

Scintillators are the “eyes” of scanners in positron emission tomographs which deliver information on each photon, e.g. exact location, time of transformation in the detector and energy. Therefore the choice of the scintillation material, surface treatment and reflector type affect the kinetics, energy and spatial resolutions of the detector [1]. The sensitive part of the detector is high optical quality single crystals [2].

The necessity of high-quality imaging imposes the following requirements onto the sensitive crystals of detectors [1, 3–7]:

- high density of the scintillation material for ensuring a high braking capacity for radiation with respective energies and high efficiency of ionizing radiation absorption;
- high light yield for improvement of the optical and spatial resolution of detection systems and the image noise reduction at low signal levels;
- fast scintillation rise and decay time;
- radiation hardness;
- high mechanical, chemical and thermal stability;
- lack of hygroscopicity;
- transparency to self-radiation for avoiding internal light scattering in the scintillator;

– compatibility with the spectral sensitivity of the photodetector;
– affordable price.

$Gd_3Al_2Ga_3O_{12}$: Ce **(GAGG : Ce)** scintillating single crystals meet the above listed requirements and therefore show good promise for medical visualization:

– high density (6.63 g/cm^3 [1]);
– high light yield ((40–60) · 10^3 photon/MeV [8, 9]);
– radiation hardness and not hygroscopic [6, 8, 9];
– their emission peak release ($\lambda_{em} \approx 520 \div 530$ nm) is very close to the sensitivity peak of Si photomultiplier at $\lambda \approx 500$ nm [4];
– transparent for their self-radiation ($\lambda_{em} \approx 520 \div 530$ nm).

Despite the above good properties the material has a disadvantage, i.e., long decay time the fast component of which is 88 ns [9]. The poor scintillation kinetics of GAGG : Ce hinder its applications. Many researchers proposed methods of improving their kinetic parameters by co-doping of the GAGG : Ce matrix [10, 11].

Most often impurities for GAGG : Ce co-doping are selected to be calcium (Ca^{2+}) [10–14] and magnesium (Mg^{2+}) [10, 15–17]. Some research teams used lithium (Li^{+}) [18], boron (B^{3+}) [11, 19] and barium (Ba^{2+}) [11] as co-doping impurities. Multiple doping of the crystals was also used, e.g. GAGG : Ce,Mg,Ti [8]. Thus the search for optimal co-doping impurities and their concentrations is still relevant.

Analysis of literary data shows that most attention is paid to the study of scintillation properties [14, 15, 17, 20] whereas there are few if any works are focused on the optical properties of co-doped GGAG : Ce. The aim of this work is to study and describe the fundamental optical properties of GGAG : Ce crystals co-doped with Ca^{2+} (GAGG : Ce,Ca) and Zr^{4+}(GAGG : Ce,Zr).

2. Experimental

The test samples GAGG : Ce,Ca and GAGG : Ce,Zr were grown by Cz method in iridium crucibles in an argon atmosphere with 1–2% oxygen at JSC Fomos-Materials. The charge was specially synthesized from pure (99.99%) oxides of the respective elements. The crystals were grown in the (100) direction and high-temperature annealed at 1400 °C in air. The test samples with thickness $d \sim 0.2$ cm were cut perpendicularly to the growth axis and double-side polished.

The optical properties of the crystals were studied at the accredited testing laboratory «Single Crystals and Stock on Their Base» of the National University of Science and Technology «MISiS» using certified spectrophotometric techniques on verified equipment. The accuracy and stability of the results were checked using reference specimens samples [21].

The transmission coefficient spectra for normally incident naturally polarized light were taken on a Cary 5000 spectrophotometer in the 200–2200 nm. An automatic universal measurement accesory (UMA, Agilent Technologies) was used for determination of the reflection indices of *p*-polarized light (R_p, %) for different incidence angles including the Brewster angle.

The absorption coefficient α, cm^{-1}, was determined for a wide spectral range from UV to IR (200–2200 nm) [22] in accordance with the Bouguer-Lambert law on the base of measured transmission coefficient spectra (T,%):

$$\alpha = \frac{\ln\left(\frac{1}{T}\right)}{d}, \quad (1)$$

The refractive index *n* was determined using the Brewster spectrophotometric method for which the reflection intensity of *p*-polarized light equals zero at the Brewster angle.

To determine the refractive index with the Brewster method we took the angle reflection spectra for *p*-polarized light at different incidence angles in the 400–600 nm. The incidence angle was varied from 50° to 75° with 5° steps. Then we determined the angle at which the reflection coefficient was the lowest. Finally we obtained a more accurate Brewster angle by iteration (reducing the step to 0.05°) and acquiring statistical data [23].

The refractive index *n* for a specific wavelength was calculated from the Brewster angle φ_{Br} found as described above using the formula [22, 24]:

$$\mathrm{tg}\ \varphi_{Br} = n. \quad (2)$$

The Brewster method can be used for the determination of ordinary refractive index. The data on *n* obtained using this formula are discrete and plotting a dispersion curve requires special approximating equations [25].

The Brewster method does not require any special sample shape, the only condition is one polished face since the refractive index calculated by this method does not depend on reflected light intensity. Nevertheless this method is labor consuming and requires acquisition of statistical data and their metrological computation. The Brewster method guarantees refractive index determination accurate to 3 decimal places as was shown by metrological tests for reference samples [26].

3. Results and discussion

The transmission coefficient spectra for normally incident light were taken and the absorption coefficient was assessed in the 200–2200 nm for all the samples.

The data shown in Fig. 1 indicate that the transmission coefficient spectra are nonmonotonic at up to 600 nm wavelengths. Absorption bands above 600 nm are not observed. Therefore Fig. 2 shows absorption spectra for the GAGG : Ce; GAGG : Ce,Ca and GAGG:Ce,Zr crystals calculated using Eq. (1) at 200–600 nm . The data suggest that co-doping of the GAGG : Ce crystal matrix affects the transmittance of the crystals as follows:

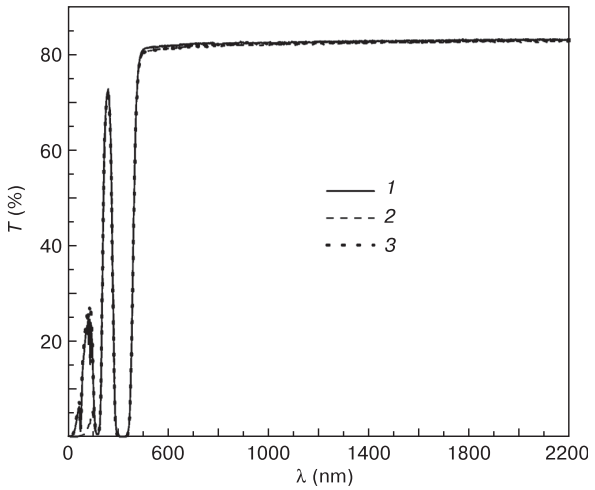

Figure 1. Transmittance spectra of (*1*) GAGG : Ce; (*2*) GAGG : Ce,Ca and (*3*) GAGG : Ce,Zr crystals.

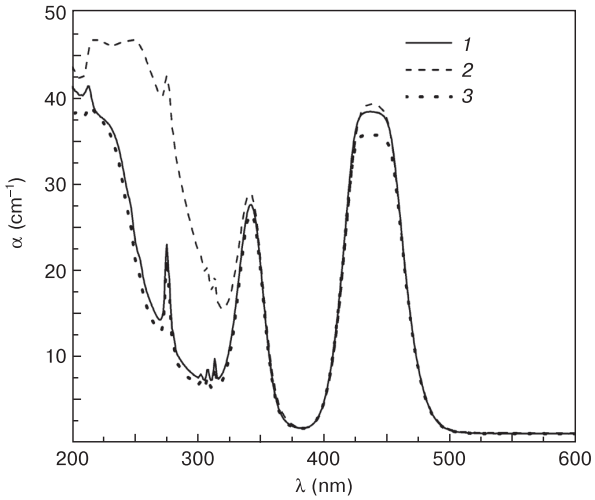

Figure 2. Absorption spectra of (*1*) GAGG : Ce; (*2*) GAGG : Ce,Ca and (*3*) GAGG : Ce,Zr crystals.

– Zr^{4+} impurity slightly increases the short-wave transmittance;
– Ca^{2+} impurity decreases the short-wave transmittance.

The data shown in Fig. 2 suggest that the α(λ) spectra of all the test crystals are nonmonotonic and contain prominent strong absorption bands. For example (Fig. 2) there are two bands at 340 and 440 nm corresponding to 4*f*–5*d* Ce^{3+} level electron transitions and bands at 230 and 270 nm, as well as a region of bands near ~310 nm corresponding to Gd^{3+} level electron transitions [27]. Obviously, Ca^{2+} and Zr^{4+} co-doping of GAGG : Ce crystals did not shift the absorption bands but only changed the absorption intensity.

The absorption coefficient of the crystals after Ca^{2+} co-doping increased in the short-wave region which does not contradict to earlier results [11]. There is a hypothesis [10, 12] that the increase in the absorption was caused by Ce^{4+} formation due to Ce^{3+} recharging.

Unlike Ca^{2+} the presence of Zr^{4+} has a smaller effect on the absorption in the crystals. However the absorption intensity at the widest cerium band (440 nm) is lower than that for GAGG : Ce.

GAGG : Ce single crystals have a cubic structure with the *Ia3d* space symmetry group [20]. These crystals are isotropic and have one refractive index *n* for each wavelength [28].

To calculate *n* with the Brewster method we took reflection spectra for *p*-polarized light at different incidence angles (Fig. 3). The characteristic incidence angles for refractive index estimation in dielectrics are above 50°. We searched for the Brewster angle at 50–70° with a 5° step.

The intensity of the reflection spectra decreased with an increase in the light incidence angle up to ~60° but with a further increase in the incidence angle the light intensity increased. The experimental spectra suggest that the reflection intensity at a ~60° incidence angle is the minimum one and hence the Brewster angle is near this angle.

To obtain exact φ_{Br} we iterated the reflection coefficient R_p by reducing the step to 0.05°. After reaching the lowest R_p we multiply repeated the measurements to acquire more statistical data and thus improve φ_{Br} accuracy. We carried out similar measurements for different wavelength at 300–650 nm. To obtain dispersion curves we approximated the experimental refractive index *n* using the Cauchy, Hartmann, Sellmeier etc. equations. The Cauchy equation proved to provide for the best approximation of the refractive index:

$$n = A + \frac{B}{\lambda^2} + \frac{C}{\lambda^4} + \cdots, \quad (3)$$

where *A*, *B* and *C* are the material constants of the equation.

The GAGG : Ce dispersion of refractive indices was estimated earlier using two spectrophotometric methods [27, 29]. Comparing the refractive indices of the initial

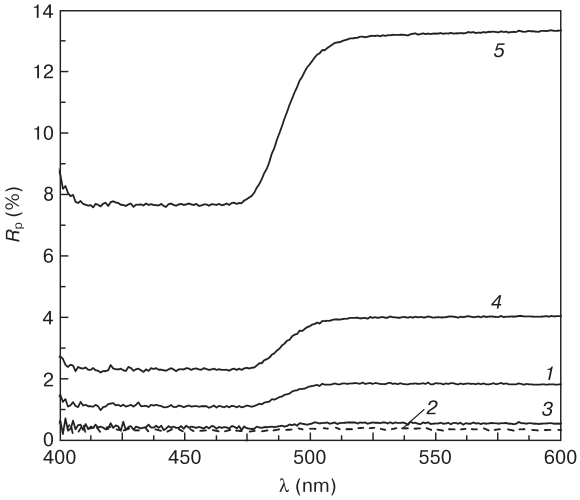

Figure 3. Angular dependences of reflection coefficient of *p*-polarized light at different incidence angles: (*1*) 55°; (*2*) 60°; (*3*) 65°; (*4*) 70°; (*5*) 75°.

composition crystal and the data on *n* obtained in this work for the co-doped GAGG : Ce, Ca and GAGG : Ce, Zr crystals, we made the following observations:

– the refractive indices of the GAGG:Ce,Zr crystal co-doped with Zr^{4+} is lower than that of the initial composition GAGG : Ce crystal in the entire experimental range;
– the refractive indices of the co-doped GAGG : Ce,Ca crystal in the >300 nm region is also lower than that of GAGG : Ce, but in the UV region (< 300 nm) the refractive index of the calcium co-doped crystals is somewhat higher than that of GAGG : Ce.

Refractive indices of the tested crystals are summarized in Table 1. Table 2 are presened in the material constants of the Cauchy equation for each of the experimental crystals.

Table 1. Refractive indices of $Gd_3Al_2Ga_3O_{12}$: Ce and $Gd_3Al_2Ga_3O_{12}$: Ce co-doped with Ca^{2+} and Zr^{4+}

Wavelength, nm	Refractive index		
	GAGG : Ce	GAGG : Ce,Ca	GAGG : Ce,Zr
250	2,321	2,403	2,276
300	**2,074**	**2,083**	**2,032**
350	**1,984**	1,959	1,938
370	1,955	**1,938**	**1,921**
400	1,931	**1,899**	**1,905**
420	**1,922**	1,894	1,892
440	**1,908**	1,885	1,886
450	1,909	**1,881**	**1,890**
460	**1,900**	1,878	1,882
500	**1,898**	1,870	1,878
550	1,891	1,865	1,876
589	**1,889**	**1,865**	**1,875**
600	1,887	1,863	1,875
650	**1,888**	**1,863**	**1,875**

Notations: Experimental data on *n* are bolded.

Table 2. Material constants of the Cauchy equation for GAGG : Ce, GAGG : Ce,Ca and GAGG : Ce,Zr

Crystal	Material Constants of the Cauchy Equation		
	A	*B*, nm²	*C*, nm⁴
GAGG : Ce	1,89	–6000,46	$2{,}07 \times 10^9$
GAGG : Ce,Ca	1,88	–14394,91	$2{,}94 \times 10^9$
GAGG : Ce,Zr	1,90	–14617,38	$2{,}39 \times 10^9$

4. Conclusion

The optical parameters of the $Gd_3Al_2Ga_3O_{12}$: Ce scintillation single crystals were determined using optical spectroscopy at 200–2200 nm and the effect of co-doping with Ca^{2+} and Zr^{4+} on these parameters was described. The transmission coefficient spectra of the test samples (GAGG:Ce and co-doped crystals) are nonmonotonic and contain typical absorption bands peaking at $\lambda \approx 440$, 340, 300–310, 270 and 230 nm. Co-doping with Ca^{2+} (the GAGG : Ce, Ca crystal) significantly increases the absorption coefficient in the short-wave region. The effect of Zr^{4+} impurity proves to be smaller than that of Ca^{2+}.

The refractive indices of GAGG : Ce,Ca and GAGG : Ce,Zr were for the first time obtained using the Brewster spectrophotometric method. The $n(\lambda)$ dispersion dependences of these materials were plotted using the Cauchy approximation equation and the material constants of this equation were determined.

We show that the refractive indices of the GAGG : Ce,Zr and GAGG : Ce,Ca crystals are lower in the experimental wavelength range (> 300 nm) than those of GAGG : Ce. In the UV region the refractive indices of the GAGG : Ce,Ca crystal are slightly higher than those of GAGG : Ce.

Acknowledgments

This work was financially supported by the Ministry of Science and Higher Education of the Russian Federation within the framework of the State Assignment to the University No. 3.2794.2017/PCh, No. 11.5583.2017/Engineering (11.5583.2017/7.8), No. 11.6181.2017/Engineering (11.6181.2017/7.8). The studies was carried out at the Interdepartmental Educational Testing Laboratory of Semiconductor and Dielectric Materials «Single Crystals and Stock on their Base» of the National University of Science and Technology «MISiS».

The authors are gratefull to A.P. Kozlova (NUST "MISiS") for the assistance during spectrophotometric measurements.

References

1. Stewart A.G., Seitz B., O'Neill K., Wall L., Jackson J.C. Energy resolution of Ce : GAGG and Pr : LuAG scintillators coupled to 3 mm × 3 mm silicon photomultipliers. *IEEE Transactions on Nuclear Science*, 2016; 63(5): 2496–2501. https://doi.org/10.1109/TNS.2016.2574773
2. Yanagida T., Kamada K., Fujimoto Y., Yagi H., Yanagitani T. Comparative study of ceramic and single crystal Ce : GAGG scintillator. *Optical Materials*, 2013; 35(12): 2480–2485. https://doi.org/10.1016/j.optmat.2013.07.002
3. Lecoq P. Development of new scintillators for medical applications. *Nuclear Instruments and Methods in Physics Research Section A: Accelerators, Spectrometers, Detectors and Associated Equipment*, 2016; 809: 130–139. https://doi.org/10.1016/j.nima.2015.08.041
4. Seitz B., Stewart A.G., O'Neill K., Wall L., Jackson C. Performance evaluation of novel SiPM for medical imaging applications. *IEEE Nuclear Science Symposium and Medical Imaging Conference (NSS/MIC)*, 2013: 1–4. https://doi.org/10.1109/NSSMIC.2013.6829685

5. Kamada K., Shimazoe K., Ito S., Yoshino M., Endo T., Tsutsumi K., Kataoka J., Kurosawa S., Yokota Y., Takahashi H., Yoshikawa A. Development of a prototype detector using APD-arrays coupled with pixelized Ce: GAGG scintillator for high resolution radiation imaging. *IEEE Transactions on Nuclear Science*, 2014; 61(1): 348–352. https://doi.org/10.1109/TNS.2013.2290319
6. Yeom J.Y., Yamamoto S., Derenzo S.E., Spanoudaki V.C., Kamada K., Endo T., Levin C.S. First performance results of Ce: GAGG scintillation crystals with silicon photomultipliers. *IEEE transactions on nuclear science*, 2013; 60(2): 988–992. https://doi.org/10.1109/TNS.2012.2233497
7. Hanin V.M. *Stsintillyatsionnyye protsessy v aktivirovannykh tseriyem keramikakh so strukturoy granata* [Scintillation processes in cerium-activated ceramics with garnet structure]: diss. PhD in phys.-math. sci. St. Petersburg, 2017, 173 p. (In Russ.)
8. Alenkov V., Buzanov O., Dosovitskiy G., Egorychev V., Fedorov A., Golutvin A., Guz U., Jacobsson R., Korjik M., Kozlov D., Mechinsky V., Schopper A., Semennikov A., Shatalov P., Shmanin E. Irradiation studies of a multi-doped $Gd_3Al_2Ga_3O_{12}$ scintillator. *Nuclear Instruments and Methods in Physics Research Section A: Accelerators, Spectrometers, Detectors and Associated Equipment*, 2019; 916: 226–229. https://doi.org/10.1016/j.nima.2018.11.101
9. Oshima T., Kataoka J., Kishimoto A., Fujita T., Kurei Y., Nishiyama T., Morita H., Yamamoto S., Ogawa K. Development of a high-precision color gamma-ray image sensor based on TSV-MPPC and diced scintillator arrays. *Nuclear Instruments and Methods in Physics Research Section A: Accelerators, Spectrometers, Detectors and Associated Equipment*, 2015; 803: 8–14. https://doi.org/10.1016/j.nima.2015.08.068
10. Nikl M., Yoshikawa A. Recent R&D trends in inorganic single-crystal scintillator materials for radiation detection. *Advanced Optical Materials*, 2015; 3(4): 463–481. https://doi.org/10.1002/adom.201400571
11. Meng F. *Development and Improvement of Cerium Activated Gadolinium Gallium Aluminum Garnets Scintillators for Radiation Detectors by Codoping*: PhD diss. Knoxville, 2015, 159 p.
12. Wu Y., Meng F., Li Q. Koschan M., Melcher C.L. Role of Ce^{4+} in the scintillation mechanism of codoped $Gd_3Ga_3Al_2O_{12}$: Ce. *Phys. Rev. Appl*., 2014; 2(4): 044009. https://doi.org/10.1103/PhysRevApplied.2.044009
13. Meng F., Koschan M., Wu Y., Melcher C. L. Relationship between Ca^{2+} concentration and the properties of codoped $Gd_3Ga_3Al_2O_{12}$:Ce scintillators. *Nuclear Instruments and Methods in Physics Research Section A: Accelerators, Spectrometers, Detectors and Associated Equipment*, 2015; 797: 138–143. https://doi.org/10.1016/j.nima.2015.06.043
14. Tyagi M., Rothfuss H.E., Donnald S.B., Koschan M., Melcher C.L. Effect of Ca^{2+} co-doping on the scintillation kinetics of Ce doped $Gd_3Ga_3Al_2O_{12}$. *IEEE Transaction on Nuclear Science*, 2014; 61(1): 297–300. https://doi.org/10.1109/TNS.2013.2276101
15. Yoshino M., Kamada K., Shoj Y., Yamaji A., Kurosawa S., Yokota Y., Ohashi Y., Yoshikawa A., Chani V.I. Effect of Mg co-doping on scintillation properties of Ce : $Gd_3(Ga, Al)_5O_{12}$ single crystals with various Ga/Al ratios. *J. Crystal Growth*, 2017; 468: 420–423. https://doi.org/10.1016/j.jcrysgro.2016.12.054
16. Babin V., Bohacek P., Grigorjeva L., Kucera M., Nikl M., Zazubovich S., Zolotarjovs A. Effect of Mg^{2+} ions co-doping on luminescence and defects formation processes in $Gd_3(Ga,Al)_5O_{12}$: Ce single crystals. *Optical Materials*, 2017; 66: 48–58. https://doi.org/10.1016/j.optmat.2017.01.039
17. Lucchini M.T., Babin V., Bohacek P., Gundacker S., Kamada K., Nikl M., Petrosyan A., Yoshikawa A., Auffray E. Effect of Mg^{2+} ions co-doping on timing performance and radiation tolerance of Cerium doped $Gd_3Al_2Ga_3O_{12}$ crystals. *Nuclear Instruments and Methods in Physics Research Section A: Accelerators, Spectrometers, Detectors and Associated Equipment*, 2016; 816: 176–183. https://doi.org/10.1016/j.nima.2016.02.004
18. Kamada K., Shoji Y., Kochurikhin V. V., Yoshino M., Okumura S., Yamamoto S., Yeom J. Y., Kurosawa S., Yokota Y., Ohashi Y., Nikl M., Yoshino M., Yosikawa A. 2-inch size Czochralski growth and scintillation properties of Li^+ co-doped Ce:$Gd_3Ga_3Al_2O_{12}$. *Optical Materials*, 2017; 65: 52–55. https://doi.org/10.1016/j.optmat.2016.09.005
19. Rawat S., Tyagi M., Netrakanti P.K., Kashyap V.K.S., Mitra A., Singh A.K., Desai D.G., Kumar G.A., Gadkari S.C. Pulse shape discrimination properties of $Gd_3Ga_3Al_2O_{12}$: Ce, B single crystal in comparison with CsI: Tl. *Nuclear Instruments and Methods in Physics Research Section A: Accelerators, Spectrometers, Detectors and Associated Equipment*, 2016; 840: 186–191. https://doi.org/10.1016/j.nima.2016.09.060
20. Kamada K., Yanagida T., Endo T., Tsutumi K., Usuki Y., Nikl M., Fujimoto Y., Yoshikawa A. 2-inch size single crystal growth and scintillation properties of new scintillator; Ce: $Gd_3Al_2Ga_3O_{12}$. *Nuclear Science Symposium and Medical Imaging Conference (NSS/MIC)*, 2011: 1927–1929. https://doi.org/10.1109/NSSMIC.2011.6154387
21. Kozlova N.S., Goreeva Zh. A., Zabelina Ev. V. Testing quality assurance of single crystals and stock on their base. *IEEE 2nd Internat. Ural Conf. on Measurements (UralCon)*. Chelyabinsk (Russia), 2017: 15–22. https://doi.org/10.1109/URALCON.2017.8120681
22. Landsberg G. S. *Optika* [Optics]. Moscow: Nauka, 1976, 296 p. (In Russ.)
23. Application note. URL: https://www.agilent.com/cs/library/applications/application-refractive-index-cary-5000-uv-vis-5994-0052en-us-agilent.pdf (accessed: 15.02.2019)
24. Borisenko S.I., Revinskaya O.G., Kravchenko N.S., Chernov A.V. *Pokazatel' prelomleniya sveta i metody yego eksperimental'nogo opredeleniya* [The refractive index of light and methods of its experimental determination]. Tomsk: Tomskiy politekhnicheskiy universitet, 2014, 146 p. (In Russ.)
25. Palik E.D. *Handbook of optical constants of solids*. New York: Academic Press, 1998, 3224 p.
26. Kozlova N.S., Kozlova A.P., Goreeva Zh.A. Spectrophotometric methods and their capabilities to study material optical parameters. *IEEE 2nd International Ural Conference on Measurements (UralCon)*, 2017: 281–288. https://doi.org/10.1109/URALCON.2017.8120724
27. Kozlova N.S., Buzanov O.A., Kasimova V.M., Kozlova A.P., Zabelina E.V. Optical characteristics of single crystal $Gd_3Al_2Ga_3O_{12}$: Ce. *Modern Electronic Materials*, 2018; 4(1): 7–12. https://doi.org/10.3897/j.moem.4.1.33240
28. Perelomova N.V., Tagieva M.M. *Krystallofizika* [Crystal Physics]. Moscow: NUST MISiS, 2013, 408 p. (In Russ.)
29. Kozlova N.S., Busanov O.A., Zabelina E.V., Kozlova A.P., Kasimova V.M. Optical properties and refractive indices of $Gd_3Al_2Ga_3O_{12}$: Ce^{3+} crystals. *Crystallography Reports*, 2016; 61(3): 474–478. https://doi.org/10.1134/S1063774516030160